JNS PEDIATRICS

LABORATORY INVESTIGATION

J Neurosurg Pediatr 19:518–530, 2017

Preclinical evaluation of convection-enhanced delivery of liposomal doxorubicin to treat pediatric diffuse intrinsic pontine glioma and thalamic high-grade glioma

A. Charlotte P. Sewing, MD,[1,3,4] Tonny Lagerweij, MSc,[2–4] Dannis G. van Vuurden, MD, PhD,[1,3,4] Michaël H. Meel, MD,[1,2,4] Susanna J. E. Veringa, MD,[1,3,4] Angel M. Carcaboso, PhD,[9] Pieter J. Gaillard, PhD,[5] W. Peter Vandertop, MD, PhD,[2,4] Pieter Wesseling, MD, PhD,[3–7] David Noske, MD, PhD,[2–4] Gertjan J. L. Kaspers, MD, PhD,[3,8] and Esther Hulleman, PhD[1,3,4]

Departments of [1]Pediatric Oncology, [2]Neurosurgery, and [6]Pathology; [3]Neuro-Oncology Research Group; [4]Brain Tumor Center Amsterdam, VU University Medical Center, Amsterdam; [5]2-BBB Medicines, Leiden; [7]Department of Pathology, RadboudUMC, Nijmegen; [8]Academy of Princess Máxima Center for Pediatric Oncology, Utrecht, The Netherlands; and [9]Preclinical Therapeutics and Drug Delivery Research Program, Department of Oncology, Hospital Sant Joan de Déu Barcelona, Spain

OBJECTIVE Pediatric high-grade gliomas (pHGGs) including diffuse intrinsic pontine gliomas (DIPGs) are primary brain tumors with high mortality and morbidity. Because of their poor brain penetrance, systemic chemotherapy regimens have failed to deliver satisfactory results; however, convection-enhanced delivery (CED) may be an alternative mode of drug delivery. Anthracyclines are potent chemotherapeutics that have been successfully delivered via CED in preclinical supratentorial glioma models. This study aims to assess the potency of anthracyclines against DIPG and pHGG cell lines in vitro and to evaluate the efficacy of CED with anthracyclines in orthotopic pontine and thalamic tumor models.

METHODS The sensitivity of primary pHGG cell lines to a range of anthracyclines was tested in vitro. Preclinical CED of free doxorubicin and pegylated liposomal doxorubicin (PLD) to the brainstem and thalamus of naïve nude mice was performed. The maximum tolerated dose (MTD) was determined based on the observation of clinical symptoms, and brains were analyzed after H & E staining. Efficacy of the MTD was tested in adult glioma E98-FM-DIPG and E98-FM-thalamus models and in the HSJD-DIPG-007-Fluc primary DIPG model.

RESULTS Both pHGG and DIPG cells were sensitive to anthracyclines in vitro. Doxorubicin was selected for further preclinical evaluation. Convection-enhanced delivery of the MTD of free doxorubicin and PLD in the pons was 0.02 mg/ml, and the dose tolerated in the thalamus was 10 times higher (0.2 mg/ml). Free doxorubicin or PLD via CED was ineffective against E98-FM-DIPG or HSJD-DIPG-007-Fluc in the brainstem; however, when applied in the thalamus, 0.2 mg/ml of PLD slowed down tumor growth and increased survival in a subset of animals with small tumors.

CONCLUSIONS Local delivery of doxorubicin to the brainstem causes severe toxicity, even at doxorubicin concentrations that are safe in the thalamus. As a consequence, the authors could not establish a therapeutic window for treating orthotopic brainstem tumors in mice. For tumors in the thalamus, therapeutic concentrations to slow down tumor growth could be reached. These data suggest that anatomical location determines the severity of toxicity after local delivery of therapeutic agents and that caution should be used when translating data from supratentorial CED studies to treat infratentorial tumors.

https://thejns.org/doi/abs/10.3171/2016.9.PEDS16152

KEY WORDS convection-enhanced delivery; CED; diffuse intrinsic pontine glioma; DIPG; pediatric high-grade glioma; pHGG; thalamus; doxorubicin; anthracyclines; oncology

ABBREVIATIONS BBB = blood-brain barrier; BLI = bioluminescent imaging; CED = convection-enhanced delivery; DIPG = diffuse intrinsic pontine glioma; GBM = glioblastoma multiforme; IC50 = half maximal inhibitory concentration; LG-BSG = low-grade brainstem glioma; MTD = maximum tolerated dose; PBS = phosphate-buffered saline; pHGG = pediatric high-grade glioma; PLD = pegylated liposomal doxorubicin; TOPIIA = topoisomerase Type IIA; VUMC = VU University Medical Center.

SUBMITTED March 11, 2016. **ACCEPTED** September 27, 2016.
INCLUDE WHEN CITING Published online February 17, 2017; DOI: 10.3171/2016.9.PEDS16152.

DIFFUSE intrinsic pontine glioma (DIPG) and thalamic glioma are diffusely infiltrating midline gliomas, often harboring histone H3K27M mutations and most frequently observed in childhood.[47] These tumors have very high mortality and morbidity as effective treatment strategies still do not exist,[18,26] despite significant progress in understanding the biological processes that play a role in the development and progression of these tumors.[7,8,22,36,53] Tumor cells are highly resistant to chemo- and radiotherapy, and the presence of the blood-brain barrier (BBB) prevents drugs from reaching the bulk tumor and infiltrating tumor cells in sufficient concentrations.[24,43]

None of the clinical trials performed in DIPG and pediatric high-grade glioma (pHGG), which have used a large number of different chemotherapeutic agents such as cytostatic agents, targeted antibodies, and small-molecule inhibitors, has yet to show a clear benefit that can be translated to standard clinical practice.[27,36] Recently, preclinical research has identified pHGG and DIPG cell lines to be sensitive to a number of "classic" cytostatic agents, especially some anthracycline drugs.[50] Anthracyclines are the cornerstones of many chemotherapeutic treatment regimens in a wide variety of cancer types in both adults and children.[48] They are, despite their assumed value, associated with serious adverse events, including debilitating or even life-threatening cardiotoxicity.[33] Almost all anthracyclines have been identified as strong substrates of ATP-binding cassette transporters (ABC transporters) P-gP, MRP1, and BCRP, causing limited brain penetration.[17,40] The limited brain penetrance of anthracyclines in brain tumors with an intact BBB, such as diffuse gliomas, may also explain these agents' lack of efficacy when used in the treatment of pHGG including DIPG.

Convection-enhanced delivery (CED) is a local delivery technique that is being considered a potential drug delivery strategy in DIPG and other brain tumors as it circumvents the BBB.[2,4,13,35,42,49] Drug distribution is facilitated by a pressure gradient at the tip of the infusion catheter, resulting in bulk flow through the interstitial spaces of the brain.[5,34] However, choosing the right drug to administer via CED is difficult: it should be effective against pHGG cells, have favorable chemical properties to enable adequate distribution, and give no or limited toxicity in healthy brain tissue.[5,34,41] Using liposomal formulations of a drug can potentially improve distribution, bioavailability, biological half-life, and efficacy after CED, as suggested by several preclinical studies.[1,30,31,55]

In the present study we aimed to investigate the translational potential of anthracyclines in the treatment of DIPG and pHGG using CED. Preclinical animal studies have already shown the potential for local delivery of anthracyclines to treat brain tumor models, but no study has investigated the administration of these chemotherapeutic drugs directly to the pons or thalamus.[30,31] We studied the efficacy of different anthracyclines in vitro and determined the feasibility of delivering these agents to delicate brain areas such as the brainstem and thalamus. Subsequently, we investigated the efficacy of nanoliposomal and free anthracyclines in treating orthotopic high-grade tumors in the brainstem and thalamus in vivo.

Methods

Expression of Topoisomerase Type IIA in DIPG and pHGG

Because topoisomerase Type IIA (TOPIIA) expression is associated with a good clinical response to treatment with anthracyclines in a number of cancer types,[15,16] *TOPIIA* mRNA expression in DIPG (n = 27[38]) and pHGG (n = 53[39]) was determined in silico by using publicly available data sets and compared with a data set of nonmalignant brain tissue (44 tissue samples[25]), low-grade brainstem glioma (LG-BSG; 6 samples[38]), and adult HGG (284 samples[23]). These data sets included tumor material from biopsy (adult and pediatric HGG and DIPG), resection (adult and pediatric HGG), and autopsy (DIPG). All expression analyses were performed using R2, a web-based microarray analysis and visualization platform (http://r2.amc.nl).

Processing of Tumor Material and Cell Cultures

Single-cell cultures were established from biopsy samples derived from pediatric glioblastoma multiforme (GBM), anaplastic astrocytoma, anaplastic oligodendroglioma, and DIPG. Informed consent was obtained according to institutionally approved protocols. Tumor pieces were collected into DMEM (PAA Laboratories GmbH) and washed twice with phosphate-buffered saline (PBS) to remove blood clots. Samples were sliced into small (3–5 mm^3) pieces and either mechanically dissociated by filtering through a cell strainer (BD Falcon Biosciences) or dissociated by incubation with Accutase (PAA Laboratories GmbH). Single cells were seeded in DMEM-F12 constituted with stable glutamine, 10% fetal bovine serum (Perbio Science Nederland B.V.), 1% penicillin-streptomycin (PAA Laboratories GmbH), and 0.5% sodium pyruvate. For primary astrocytes, 15% fetal bovine serum was used. Cells were grown at 37°C in a 5% CO_2 humidified atmosphere. Primary cell cultures were genetically characterized using karyotyping or array comparative genomic hybridization (CGH), as previously described by Veringa et al.[50] The primary HSJD-DIPG-007 cell line was established from DIPG material obtained at Hospital Sant Joan de Déu (Barcelona, Spain) from a 6-year-old patient after autopsy and was confirmed to have an H3F3A (K27M) and ACVR1 (R206H) mutation.[6] The HSJD-DIPG-007-Fluc was cultured in serum-free tumor stem medium, as previously described.[28]

Drug Treatment

The primary pediatric glioma and astrocyte cultures were exposed to different anthracycline drugs (idarubicin, epirubicin, mitoxantrone, doxorubicin, and daunorubicin) at concentrations ranging from 0.01 to 1000 nM. A total of 1500 cells were seeded per well in 96-well tissue culture plates. After 96 hours, cell survival was assessed with the Acumen eX3 laser cytometer (TTO Labtech) using 300 mM of DAPI (Sigma-Aldrich) as readout. Results were analyzed using Acumen Explorer software, calculating the survival percentage for each compound tested in the assay. Each experiment was performed at least 4 times.

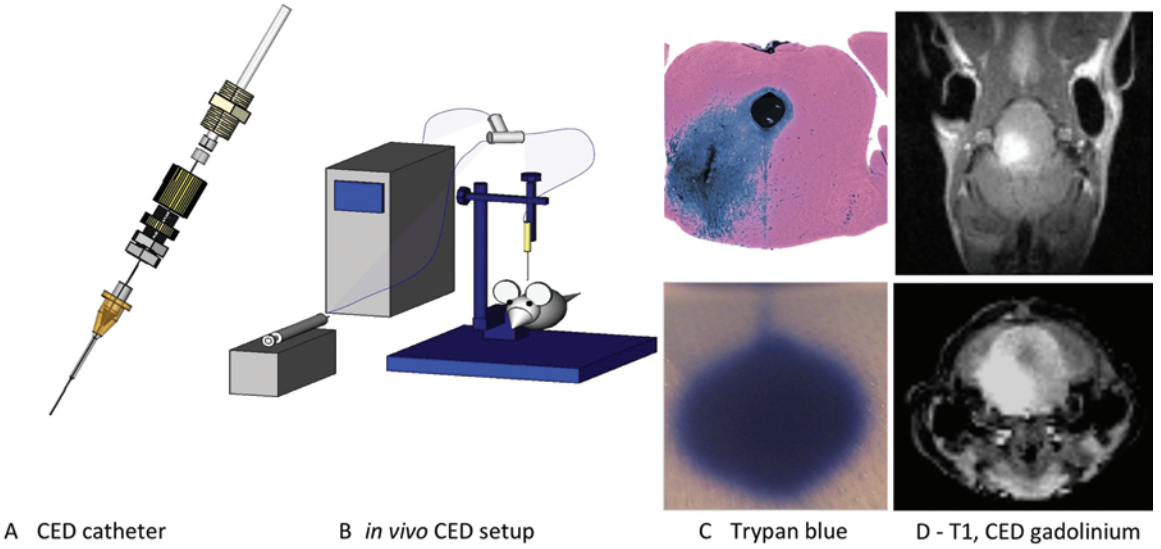

FIG. 1. Schematic overview of preclinical CED including CED catheter (**A**) and stereotactic infusion setup (**B**). Infusion of 15 µl of trypan blue to the selected stereotactic coordinates (**C**, upper) and in agarose gel (**C**, lower). T1-weighted MR images (**D**) obtained directly after infusion of 15 µl of gadolinium. Panels A, B, and C reprinted from Sewing et al: *J Neurosci Methods 238*:88–94, 2014. Published with permission. Figure is available in color online only.

Drugs

Clinical formulations of the idarubicin, epirubicin, and daunorubicin used for the in vitro drug screens were supplied by the Department of Pharmacology of the VU University Medical Center (VUMC). Free and pegylated liposomal doxorubicin (PLD) were supplied by 2-BBB Medicines BV. The PLD was prepared according to the commercial Doxil/Caelyx preparation method, that is, using active doxorubicin loading against an ammonium sulfate gradient, as previously described.[21] Mean liposome size was 95 nm and contained 2 mg/ml of doxorubicin, more than 90% of which was encapsulated in the liposomes. The liposomes were stored in liposome buffer (9.4% sucrose with histidine, 1.55 mg/ml; Sigma-Aldrich) at 4°C for no longer than 3 months after production. The vehicle was previously shown to be nontoxic in mice.[21] For details on the stability of doxorubicin and its liposomal formulation, we refer to previously published data by Barenholz and Gaillard et al.[3,21]

Animals

Animal experiments were performed in accordance with the Dutch law on animal experimentation, and the protocol was approved by the committee on animal experimentation of the VUMC. Athymic nude-foxn1^{nu} mice (6 weeks old, total of 112 mice used in all experiments) were purchased from Harlan, were kept under filter top conditions, and received food and water ad libitum.

Orthotopic DIPG Mouse Models

The E98 adult GBM cell line[14] was transduced to express firefly luciferase (Fluc) and mCherry (E98-FM cells) and cultured in DMEM supplemented with 10% fetal calf serum and penicillin-streptomycin. These cells were injected subcutaneously into female athymic nude mice (6–8 weeks of age, 1 mouse per batch of intracranially injected cells) to expand the number of cells.[9] When the subcutaneous tumor reached a diameter of 1 cm, the tumor was removed and a single-cell suspension was prepared by mechanical disruption through a 100-µm nylon cell strainer. The HSJD-DIPG-007-Fluc cells were injected directly from culture after mechanical dissociation and counting. The cells were washed once with PBS and concentrated to 10^5 cells/µl (both E98-FM and HSJD-DIPG-007-Fluc). Mice were stereotactically injected with 5×10^5 cells in a final volume of 5 µl into either the pons (x: –1.0 mm, y: –0.8 mm, and z: 4.5 mm from the lambda) or the thalamus (x: 1.5, y: –2, and z: –3.2 from the bregma). Coordinates were based on *The Mouse Brain in Stereotaxic Coordinates* by Franklin and Paxinos[20] and were previously validated using injections of trypan blue (data not shown).

Convection-Enhanced Delivery In Vivo

The CED procedure was performed using a stepped catheter specifically designed for this purpose (Fig. 1A), as we have described elsewhere.[45] In vivo targeting of the brainstem was determined by infusion of trypan blue via CED (Fig. 1C), and MRI was performed after infusion of 15 µl of gadolinium 5 µM (Dotarem, Guerbet; Fig. 1D). Imaging was performed on 3 mice anesthetized with isoflurane inhalation (1.5 L O_2/min and 2.5% isoflurane) using a preclinical PET-MRI system (nanoScan system, Mediso Medical Imaging Systems). The T1-weighted images were acquired and analyzed using MIPAV software (Medical Image Processing, Analysis, and Visualization, version 7.2.0, National Institutes of Health). To perform in vivo CED, animals were injected with buprenorphine 0.05–1 mg/kg and anesthetized with isoflurane 2%–3% in 100% O_2. After placing the animals in a stereotactic frame on a heated platform (37°C), we introduced the CED catheter into the pons (30 mice for toxicity stud-

ies, 24 mice for efficacy studies) or thalamus (9 mice for toxicity studies, 24 mice for efficacy studies; Fig. 1B). The coordinates used for CED were the same as those used for intracranial injections. During 30 minutes, a total of 15 μl of free doxorubicin, PLD, or vehicle was infused in the murine brain with a flow velocity of 0.5 μl/min. After the procedure, animals were returned to their cages to recover and resumed normal active behavior within 3–12 hours.

Toxicity Study

Convection-enhanced delivery toxicity (3 mice per dose and location) of 0.02 mg/ml (35 μM, pons), 0.2 mg/ml (345 μM, pons and thalamus), or 2 mg/ml (3448 μM, pons) of doxorubicin or PLD was determined based on clinical observations, including weight loss and clinical score. Clinical scores ranged from 0 to 4 and referred to normal active behavior (0); subtle inactivity or subtle neurological symptoms (1); mild to moderate inactivity or neurological symptoms (2); severe neurological symptoms, inactivity, loss of reflexes, and inadequate grooming (3); and death (4). Half-point scores were assigned to mice that were behaving in a manner between 2 scores. End points due to toxicity were defined as weight loss more than 15%, severe neurological symptoms, or severe inactivity. When none of these clinical end points were met, mice were euthanized 6 weeks after CED to determine histological toxicity. The maximum tolerated dose (MTD) was selected based on clinical features after treatment of 3 mice (no end point reached in all 3 animals, no clinical score > 2).

Convection-Enhanced Delivery and Intravenous Efficacy Studies

The start of treatment was determined by a rise in the bioluminescent imaging (BLI) signal, indicating tumor engraftment and growth. At Day 7 or 8 after intracranial injection of tumor cells to establish orthotopic brain tumors, mice were stratified on the basis of BLI signal intensities into different treatment groups. For the CED studies, animals harboring a pontine (E98-FM-DIPG or HSJD-DIPG-007-Fluc) or thalamic (E98-FM-thalamus) tumor were assigned to undergo CED of 0.02 mg/ml (35 μM) or 0.2 mg/ml (345 μM) of free doxorubicin or PLD, or vehicle (NaCl 0.9%; 4 mice for pons, 8 mice for thalamus per treatment group). For the intravenous studies, mice (4 per group) were assigned to receive PLD (18 mg/kg, once a week for 2 weeks) or vehicle (NaCl 0.9%) injected intravenously into the tail vein (3 mice/treatment group). Dosing was performed at the previously described MTD.[12] Follow-up included daily observations, assignment of clinical scores, and weight measurement as well as twice weekly measurement of the BLI signal (E98-FM). End points were defined as weight loss more than 15%, severe neurological symptoms, or severe inactivity. Researchers were blinded to treatment group. Mice were euthanized via pentobarbital overdose. Brains were removed and fixed in 3.7% PBS-buffered formaldehyde. Differences in survival were analyzed with Kaplan-Meier curves and log-rank tests for significance. Nonparametric Kruskal-Wallis test followed by Dunn's post hoc test was used to determine differences in the BLI signal. A p value < 0.05 was considered statistically significant.

Tissue Staining and Histological Scoring

Hematoxylin and eosin (H & E) staining was performed on 4-μm formalin-fixed, paraffin-embedded tissue sections cut in the coronal plane, using a standard H & E protocol. To determine histological toxicity in non–tumor-bearing animals, sections were selected at the site of the needle tract and 100 μm both rostrally and posteriorly. Two researchers (A.C.P.S. and T.L.) and an independent neuropathologist (P.W.) assessed tissue damage and inflammation. They were blinded to the experimental procedure that the animals underwent.

Results

Anthracyclines as Promising Drugs to Treat pHGG and DIPG

Topoisomerase Type IIA was significantly overexpressed in pHGG and DIPG as compared with levels in LG-BSG and normal brain ($p < 0.01$; Fig. 2A and B). Cytotoxicity of clinically available anthracyclines was tested in vitro against pHGG and DIPG primary cells and showed moderate to excellent sensitivity with half maximal inhibitory concentration (IC50) values ranging from 1 μM to 10 pM (Fig. 2C–G). Doxorubicin proved to be particularly active against DIPG cells (Fig. 2G). Next, the potency of doxorubicin was tested against E98-FM cells, used to establish orthotopic E98-FM-DIPG and E98-FM-thalamus models,[9,14] and normal human astrocytes, showing an excellent therapeutic window (Fig. 2H). For doxorubicin, used in subsequent in vivo experiments, IC50 values ranged from 1 nM in the VUMC-DIPG-A cell line to 0.8 μM in the VUMC-HGG-05 cell line. HSJD-DIPG-007-Fluc had an intermediate sensitivity profile (IC50 40 nM; Supplemental Fig. 2).

Clinical Toxicity of Doxorubicin Determined by Anatomical Location

Convection-enhanced delivery of high-dose (2 mg/ml) doxorubicin and PLD to the pons led to severe clinical toxicity (Fig. 3A). Severe symptoms occurred later after the CED procedure in the PLD-treated animals (6 days) than in the animals treated with free doxorubicin (1–3 days), and the difference in survival and weight loss was statistically significant ($p < 0.05$; Table 1 and Supplemental Fig. 1). Eventually, all animals treated with high-dose doxorubicin in the brainstem had to be euthanized because of unacceptable toxicity. Symptoms consisted of weight loss (> 15%) and neurological deficits including paresis and loss of balance.

Severe clinical toxicity still occurred with CED of medium-dose (0.2 mg/ml) doxorubicin to the pons. All animals in the free-doxorubicin group had to be euthanized. In the PLD group, 1 animal had to be euthanized because of severe symptoms and 1 animal had clear neurological symptoms but remained active, with weight loss within acceptable limits (< 15%); these neurological symptoms regressed after approximately 3 weeks (Table 1 and Fig. 3B).

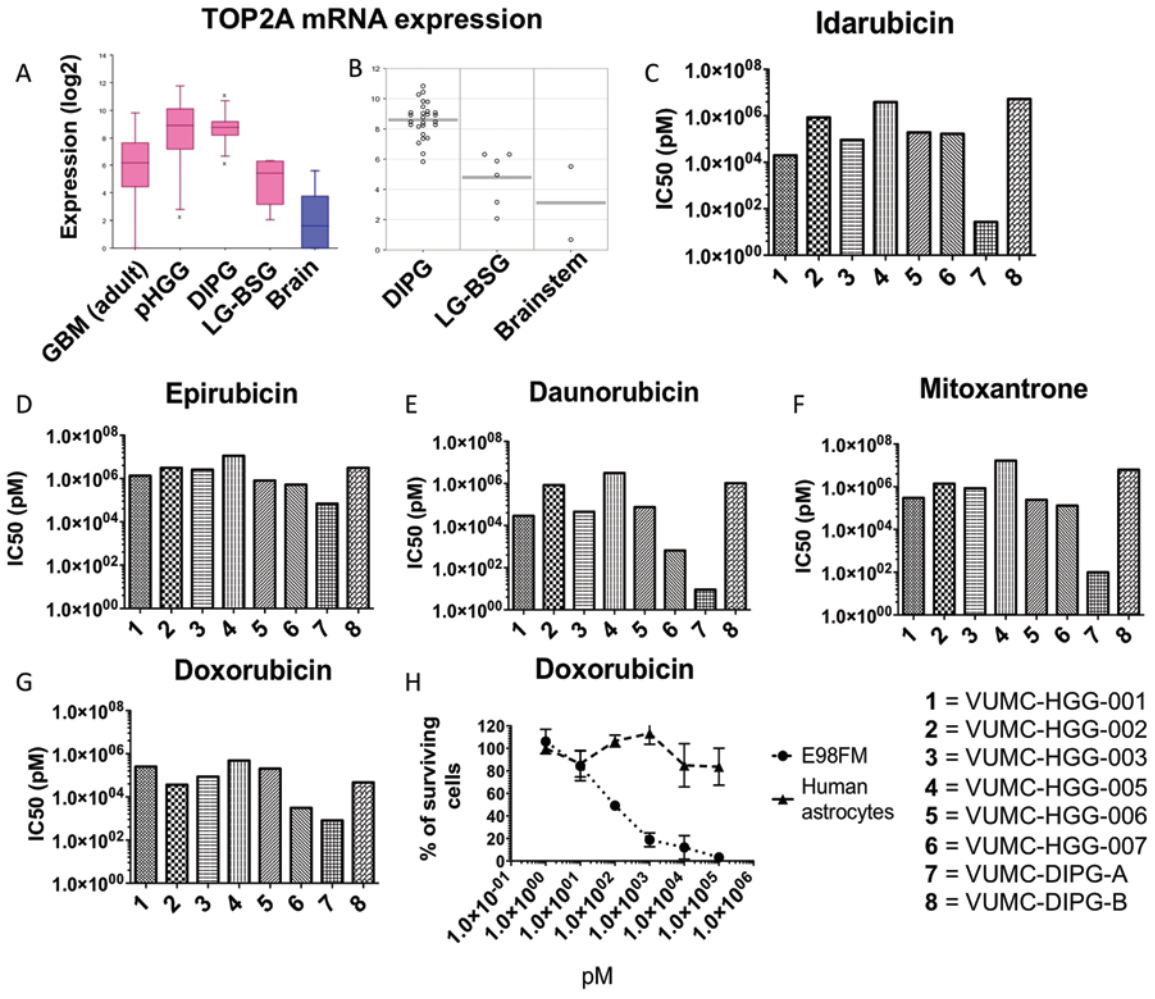

FIG. 2. Expression of TOPIIA (**A**) in adult GBM, pHGG, DIPG, LG-BSG, and normal brain. TOPIIA expression (**B**) in DIPG, LG-BSG, and normal brainstem (individual cases plotted), as assessed by mining a publicly available database (http://r2.amc.nl). Sensitivity (IC50) of pHGG and DIPG cell lines to idarubicin (**C**), epirubicin (**D**), daunorubicin (**E**), mitoxantrone (**F**), and doxorubicin (**G**). Sensitivity of normal human astrocytes and E98-FM cells to doxorubicin (**H**). Numbers 1–8 refer to VUMC-HGG and VUMC-DIPG cell lines. Figure is available in color online only.

None of the animals treated with low-dose (0.02 mg/ml) doxorubicin or PLD to the pons showed significant clinical toxicity, as illustrated by the absence of clinical symptoms after CED (data not shown). In our experience, weight loss or inadequate weight gain in the animals is a sensitive symptom of toxicity, and all animals treated with 0.02 mg/ml showed normal weight gain after treatment (Fig. 3C). To find out the MTD of doxorubicin for injection into the pons, mice were treated via CED with doses of 0.1 and 0.04 mg/ml as well. These doses still caused intolerable symptoms that were beyond the criteria set for MTD (clinical end point reached > 1 animal, clinical score > 2, data not shown).

Toxicity of CED of doxorubicin to the thalamus was significantly less pronounced. Medium-dose (0.2 mg/ml) free doxorubicin and PLD could be delivered to the thalamus without any clinical symptoms or weight loss (Fig. 3D). Given the severe toxicity seen after treatment with 2 mg/ml of doxorubicin to the pons, this dose level was not further assessed in the thalamus because of ethical considerations.

Histological Toxicity of CED Related to Dose and Formulation of Doxorubicin

After the mice were euthanized, their brains were histologically analyzed. Animals were euthanized 6 weeks after treatment unless they had to be euthanized at an earlier time point because of unacceptable clinical symptoms (CED to the pons with high- and medium-dose free doxorubicin and high-dose PLD; Table 1).

In the pons tissues obtained 6 days after high-dose (2 mg/ml) PLD treatment, we consistently noted a sharply demarcated lesion with incomplete necrosis, dispersed macrophages, and relative sparing of the microvessels (Fig. 4A). In animals treated with high-dose free doxorubicin (2 mg/ml, clinical end point reached 1–3 days after treatment), lesions were much less circumscribed and showed insipient necrosis of intervascular tissue and more widespread spongy changes of the neuropil (Fig. 4B).

In brains treated with medium-dose (0.2 mg/ml) doxorubicin to the brainstem, the tissue damage was more variable. In sharp contrast to the functional neurological

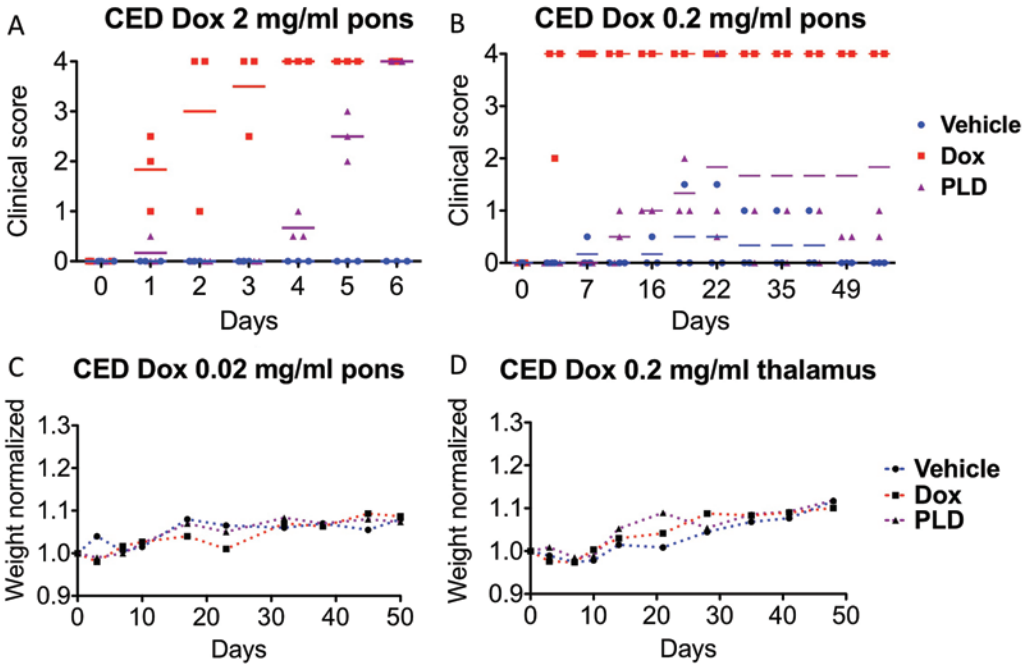

FIG. 3. Clinical symptoms of mice treated via CED of doxorubicin (Dox) in the brainstem and thalamus. Clinical scores (0–4) of mice treated with high-dose (**A**, 2 mg/ml) or intermediate-dose (**B**, 0.2 mg/ml) free doxorubicin (*red*), PLD (*purple*), or vehicle (*blue*) in the brainstem. Normalized weight gain of mice (**C**) treated with vehicle, 0.02 mg/ml of free doxorubicin, or 0.02 mg/ml PLD in the brainstem. Normalized weight gain of mice (**D**) treated with vehicle, 0.2 mg/ml of free doxorubicin, or 0.2 mg/ml of PLD in the thalamus. Figure is available in color online only.

deficits demonstrated in these animals, histological abnormalities at 2–3 days after treatment were generally absent. After treatment with 0.2 mg/ml of PLD (brains analyzed 3–6 weeks after CED), some focal gliosis and deposition of iron pigment was found (Fig. 4C).

Six weeks after treatment with low-dose (0.02 mg/ml) free doxorubicin, the brainstem showed only focal areas with more coarse texture, consistent with astrogliosis (Fig. 4D), similar to what was found in some of the animals treated with low-dose PLD or vehicle only.

After 6 weeks of follow-up, brains treated with 0.2 mg/ml of free doxorubicin to the thalamus showed clear toxicity characterized by a variably circumscribed area of tissue decay, pericellular thickening of the walls of microvessels, some iron pigment deposition (partly in macrophages), and some proliferation of (myo)fibroblasts (Fig. 4E and F). Brains treated with 0.2 mg/ml of PLD still showed similar but less pronounced lesions (Fig. 4G and H). No histological abnormalities were detected in animals treated with vehicle to the thalamus (Fig. 4I and J).

E98-FM Cells and the Formation of Diffuse Infiltrative High-Grade Tumors in the Pons and Thalamus

Adult GBM-derived E98-FM cells have been described to grow as diffuse tumors in the pons, with histological and clinical features quite similar to human DIPG.[9] To study CED in diffuse HGGs in the thalamus, we established thalamic tumors using E98-FM cells. To this end, we injected E98-FM cells into previously validated thalamic coordinates and followed in vivo tumor growth using BLI. A subset of mice injected with E98-FM to the thalamus and pons were euthanized at set time points, and their brains were analyzed to study the size and histological features of the tumors (Fig. 5A–C and G–I). Others were followed until the previously determined clinical end point (weight loss, severe neurological symptoms, or severe inactivity; Fig. 5M and N). Histological assessment showed diffuse infiltrative tumors located in the thalamus with tumor size proportionate to the bioluminescence signal. Median survival of mice with E98-FM-thalamus was 23.5 days (8 mice; Fig. 5M); for those with E98-FM-DIPG, median survival was 22 days (6 mice; Fig. 5N).

Treatment of E98-FM-DIPG and E98-FM-Thalamus With Free Doxorubicin or PLD

Both E98-FM-DIPG and HSJD-DIPG-007-Fluc, and E98-FM-thalamus tumors were treated via CED of free doxorubicin, PLD, or vehicle at the MTD determined in the previous toxicity experiments. The treatment and follow-up schedule are depicted in Fig. 6. Median survival of E98-FM-DIPG and HSJD-DIPG-007-Fluc animals treated with free doxorubicin or PLD at a low dose (0.02 mg/ml) did not differ significantly from animals treated with vehicle (Fig. 7A and G), and the bioluminescence signal was not significantly different for the E98-FM-DIPG and HSJS-DIPG-007-Fluc groups, regardless of treatment (Fig. 7B and H). Of note, 1 mouse with HSJD-DIPG-007-Fluc treated with PLD survived beyond the 90 days of follow-up. In mice with E98-FM-thalamus tumors treated with a medium dose (0.2 mg/ml), the bioluminescence signal of the tumors was significantly lower in the mice treated with PLD than in those treated with vehicle

TABLE 1. Number of days after CED that mice were euthanized because they reached the clinical end point or the end of follow-up

Location	Dose & Formulation	Euthanized After CED (days)
Pons	High	
	Doxorubicin	1–3
	PLD	5–6
	Middle	
	Doxorubicin	2–3
	PLD	20–56
	Low	
	Doxorubicin	56
	PLD	56
	Vehicle	56
Thalamus	Middle	
	Doxorubicin	56
	PLD	56
	Vehicle	56

or free doxorubicin (Fig. 7D). Survival did not differ significantly for the whole E98-FM-thalamus tumor group, regardless of treatment; however, 2 of 8 animals treated with PLD had a prolonged decrease in BLI signal and prolonged survival (Fig. 7C). Treating mice with E98-FM-DIPG tumors with intravenous PLD did not significantly influence clinical course (Fig. 7E) or bioluminescence signal (Fig. 7F).

Influence of E98-FM Tumor Size on Efficacy of PLD Treatment via CED

In the efficacy study using E98-FM-thalamus orthotopic tumors, we found a significant difference in the bioluminescence signal in the 1st week after treatment with 0.2 mg/ml PLD and noticed a survival benefit in a small proportion (2 of 8) of the mice. To determine whether this survival benefit was due to a true treatment-dependent decrease in tumor burden or just a random occurrence, we studied these animals in more detail. One noticeable difference in animals that responded to treatment was a relatively low bioluminescence signal at the start of treatment. Even though the median BLI signal was not significantly different between groups, there was great variation in the signal at the start of treatment (Fig. 8A, D, and G). We studied the response of each individual animal in relation to the bioluminescence signal at the start of treatment. Thereto, we stratified mice into low (< 10^6 photons/sec), medium (< 10^7 photons/sec), or high (> 10^7 photons/sec) tumor burden at the start of treatment. By doing so, we found that mice with E98-FM-thalamus tumors with a low tumor burden showed response to treatment with 0.2 mg/ml of PLD (Fig. 8F), while no responsive subgroup could be identified in the E98-FM-DIPG or HSJD-DIPG-007-Fluc tumors treated either via CED (PLD or doxorubicin; Fig. 8C and Supplemental Fig. 3) or intravenously (Fig. 8I). In these mice, the BLI signal rose exponentially without change, in a manner similar to that in vehicle-treated animals. This finding suggests that tumor size at the start of treatment has substantial influence on the efficacy of CED of PLD at the MTD in the thalamus but not in tumors in the pons treated at the MTD via CED or intravenously.

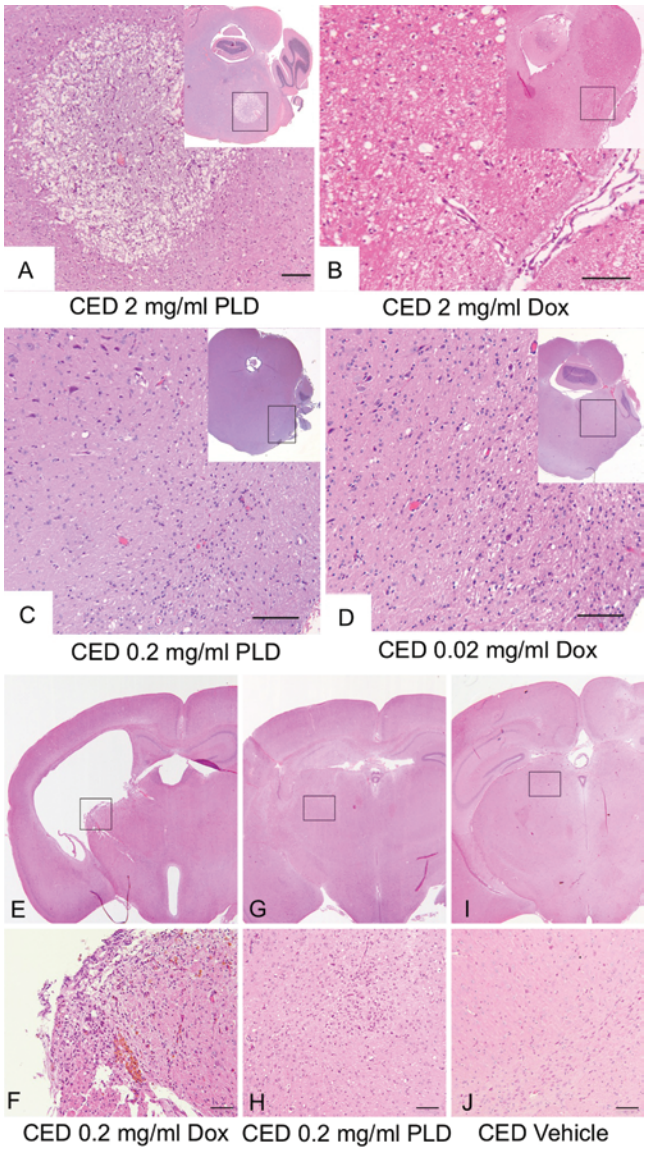

FIG. 4. *Black squares* indicate enlarged areas. Brain slices from the pontine area of mice treated with 2 mg/ml of PLD (**A**), 2 mg/ml of free doxorubicin (**B**), 0.2 mg/ml of PLD (**C**), or 0.02 mg/ml of free doxorubicin (**D**). Brain slices from the thalamic area of mice treated via CED of intermediate-dose (0.2 mg/ml) free doxorubicin (**E and F**), PLD (**G and H**), or vehicle (**I and J**). H & E. Bar = 100 μm. Figure is available in color online only.

Discussion

Using in silico and in vitro experiments, we identified anthracyclines as an interesting class of chemotherapeutics that could potentially be administered for the treatment of DIPG and pHGG. Topoisomerase Type IIA, previously shown to be correlated with anthracycline efficacy in patients,[15,16] was highly expressed in both DIPG and pHGG compared with levels in normal brain and brain-

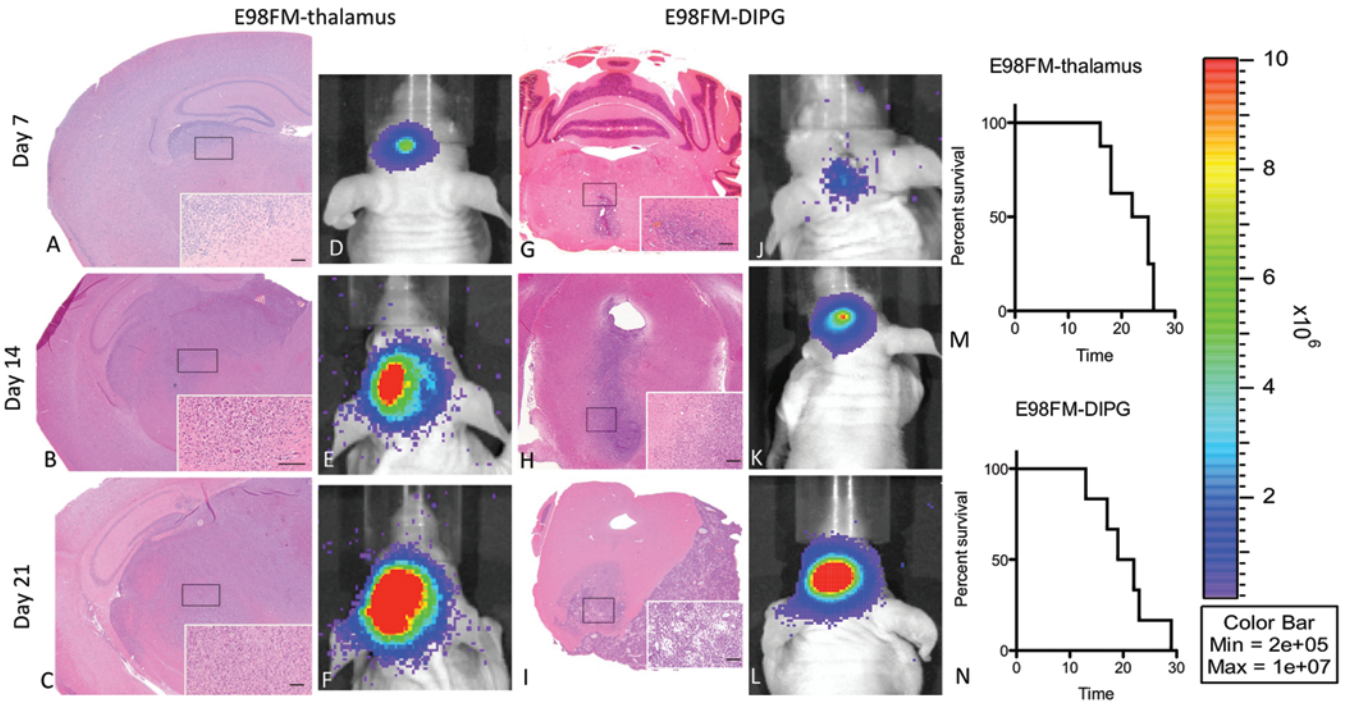

FIG. 5. Validation of the E98-FM tumor model in the pons and thalamus. Progression of E98-FM tumors after injection to the thalamus or pons at Days 7 (**A and G**), 14 (**B and H**), and 21 (**C and I**). Corresponding BLI signals (**D and J**, **E and K**, and **F and L**, respectively) and survival curves (**M and N**). Eight mice per tumor line listed. Bar = 100 μm. Figure is available in color online only.

stem. Furthermore, we showed that pHGG and DIPG cells were sensitive to anthracyclines in vitro. The severity of toxicity after local delivery via CED, however, limits effective treatment in vivo.

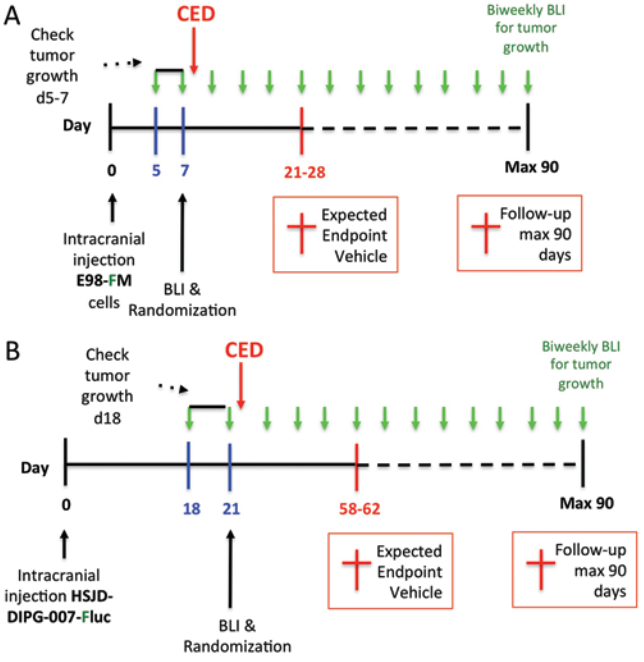

FIG. 6. Schematic of the treatment and follow-up for E98-FM-DIPG and E98-FM-thalamus (**A**) and HSJD-DIPG-007-Fluc (**B**). Figure is available in color online only.

Anthracyclines' method of action has not been fully elucidated but is thought to be multifactorial. The best-known effect of anthracycline drugs is the inhibition of TOPII, which is necessary to avoid supercoiling of DNA in dividing cells. Inhibition of TOPII leads to double-stranded breaks and subsequent cell death via apoptosis. Just a few clinical trials of anthracyclines have been conducted in children with pHGG, DIPG, or other recurrent or progressive brain tumors.[11,32,51] Results have been variable thus far. In one study, 4 of 8 patients with recurrent or progressive pHGG responded with stable disease for a period of 9–48 weeks on a regimen of PLD and oral topotecan, but the toxicity of this systemic treatment was high.[51] In another study, children with recurrent or progressive brain tumors were treated with liposomal daunorubicin, resulting in a treatment response in 6 of 14 children, with relatively mild toxicities.[32] Interestingly, our in vitro data showed that some DIPG cells (VUMC-DIPG-A) appeared to be ultrasensitive to 4 of 5 anthracyclines tested, with IC50 values well below those needed to treat all other cell lines in this panel and other glioma cell lines reported in the literature.[52] Only this particular cell line carries a mutation in histone gene *H3F3A* at lysine 27 (K27M),[22] which can be found in approximately 60% of DIPGs.[53] This mutation alters the organization of chromatin by the inability of EZH2 to trimethylate lysine 27. The absence of Lys27 trimethylation causes a more open chromatin structure and leads to gross changes in expression profiles of various cell types.[10,19,44] It was recently discovered that certain anthracyclines, including doxorubicin and daunorubicin, can cause histone eviction, especially in chromatin regions with an absence in trimethylation at lysine 27.[37]

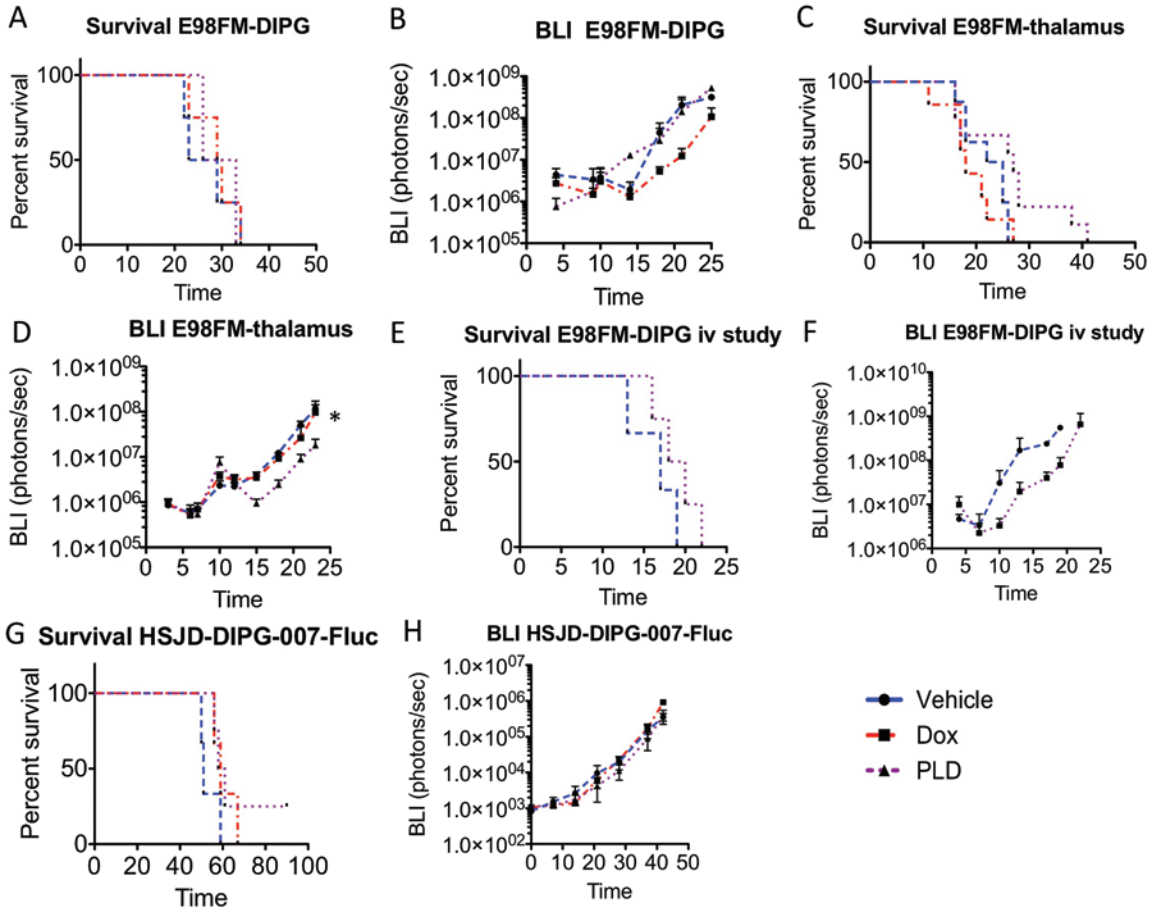

FIG. 7. Survival and corresponding BLI data of mice with E98-FM-DIPG (**A and B**) or E98-FM-thalamus (**C and D**) treated with free doxorubicin (*red*), PLD (*purple*), or vehicle (*blue*). Survival (**E**) and BLI (**F**) data of mice treated with intravenous (iv) PLD or vehicle. Survival (**G**) and BLI (**H**) data of HSJD-DIPG-007-Fluc mice treated with 0.02 mg/ml of doxorubicin, PLD, or vehicle. *$p < 0.05$. Figure is available in color online only.

This mechanism could potentially add to the sensitivity of *H3F3A*-mutated DIPG cells to anthracyclines. Further experiments to elucidate the role of histone eviction are beyond the scope of this paper. Unfortunately, the VUMC-DIPG-A cell line does not engraft after inoculation in the brain of mice and thus could not be used to perform the in vivo efficacy experiment. Therefore, another H3F3A K27M mutated cell line (HSJD-DIPG-007-Fluc), which was not part of our initial screen, was used. This cell line was intermediately sensitive to doxorubicin in vitro, but no efficacy of low-dose doxorubicin via CED could be established using our methods.

Despite their potential, these compounds' limited penetration of the brain after systemic delivery greatly constricts their clinical use in the treatment of brain tumors. In this study, we investigated the feasibility of using CED for local delivery of doxorubicin in the brainstem and thalamus. To our surprise, doxorubicin showed an MTD that was 100 times lower than the dose previously described to be safe for local delivery in the rat striatum.[30] In our experience, anatomical location clearly influenced clinical toxicity after CED. The tolerable dose when treating mice via CED of doxorubicin to the thalamus was 10 times higher than the MTD to the brainstem. Meanwhile, histological analysis of brains after CED showed similar tissue damage in the infused regions. Why this difference in toxicity occurs is not completely understood. We hypothesize that damage to the brainstem, including the pons, is more likely to produce functional deficits as compared with damage to structures in the thalamus, a phenomenon that is well known in human neurology. Of note, we only studied indirect distribution of doxorubicin by observing the spread of histological toxicity. In theory, it is possible that the distribution of free doxorubicin or PLD differs between the pons and the thalamus, causing differences in clinical presentation after CED. In this study, we also did not investigate more subtle defects in performance in mice treated with moderately high-dose doxorubicin in the thalamus. In doing so, we may have observed functional deficits that escaped our attention using basic observations. The expected tolerable dose in the thalamus still differed 10-fold from safe concentrations delivered to the striatum of rats described in the literature. Although toxicity after CED appears to be related to concentration and not total dose,[54] this finding could still be explained by the use of a relatively large volume (15 μl) compared with the volume used in most CED studies using rats (average 20 μl). Furthermore, additional toxicity could be species or even strain related.

Liposomal formulation of doxorubicin gave rise to

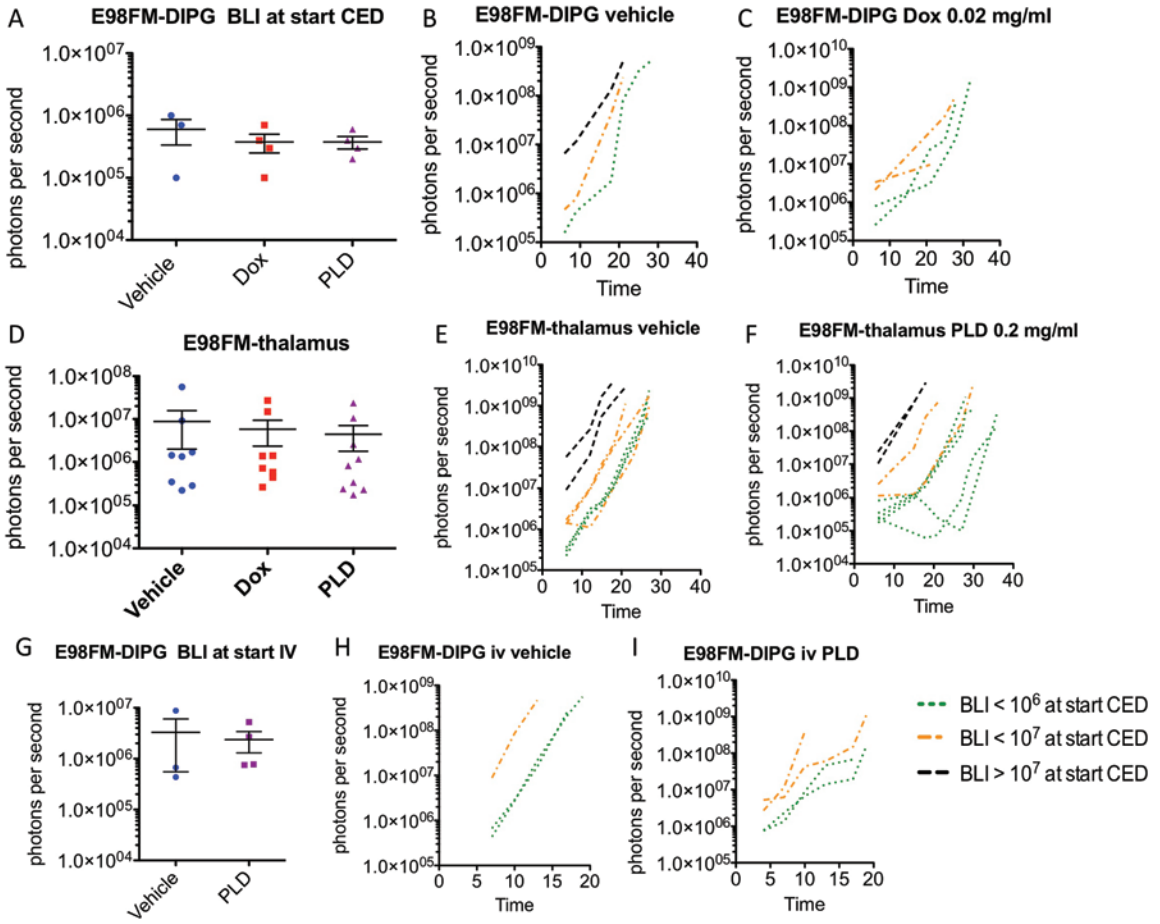

FIG. 8. Bioluminescent imaging response at the start of CED for E98-FM-DIPG (**A**) or E98-FM-thalamus (**D**) or E98-FM-iv (**G**) treated with free doxorubicin (*red*), PLD (*purple*), or vehicle (*blue*). The BLI response of individual mice was related to the bioluminescent signal at the start of CED. E98-FM-DIPG treated with vehicle (**B**) or low-dose doxorubicin (**C**), E98-FM-thalamus treated with vehicle (**E**) or intermediate-dose PLD (**F**), or intravenous (iv) administration of vehicle (**H**) or PLD (18 mg/kg once a week for 2 weeks, **I**). Figure is available in color online only.

clinical symptoms in mice much later than did the free doxorubicin, but despite this lag time, free and liposomal doxorubicin had similar MTDs. The distribution of PLD was more sphere-like, as illustrated by the circumscribed lesions found in the brains of animals treated with high doses. The high protein affinity of free doxorubicin (nearly 98%) could lead to poor distribution, and the PLD used in this study should have had a nearly ideal size (100 nm in diameter[21]) for convection through the brain interstitial spaces.[55] Our data imply that PLD indeed gives a more gradual release of doxorubicin and a wider area of distribution after CED. Both effects may enhance efficacy of CED in patients.

The low-dose doxorubicin (MTD pons) was ineffective in treating a diffusely growing orthotopic DIPG model with a single delivery, suggesting that no therapeutic window could be reached and that a one-time infusion of doxorubicin via CED would most likely have no role in the treatment of DIPG. This result is contrasted by data from our in vitro experiments showing cytotoxicity at much lower in vitro IC50 values than those delivered to tumors in vivo (up to a theoretical million-fold difference) and a substantial difference in cell survival between E98-FM and normal human astrocytes (Fig. 2H). The difference between in vitro efficacy and in vivo lack of efficacy could be attributable to inadequate coverage of the tumor due to inadequate distribution or fast efflux of doxorubicin from the brain by efflux pumps,[29] causing a much lower area under the curve than with in vitro treatment. When using the 10-fold higher dose (MTD thalamus), PLD was effective in slowing down tumor growth in the thalamus. These findings suggest that data from supratentorial CED studies cannot be directly translated to design trials to treat infratentorial tumors and stress the need for selective agents to avoid excessive toxicity to healthy surrounding tissue, especially to treat tumors in delicate areas of the brain. One preclinical study has already shown that infusing the more targeted small-molecule inhibitors dasatinib, everolimus, and perifosine can be safely performed in the rat pons using long-term CED.[56]

Using our methods, we were able to infuse a substantial area of the pons, but even when treating this area, CED was only effective when tumors were still very small. This is particularly problematic considering the

small size of the murine pons compared with the human pons. Translating this knowledge to a clinical setting would imply treating only small, very-early-stage tumors. Since this is not the clinical reality of DIPG and thalamic HGG, CED will require drugs with a very high therapeutic index or long-term continuous infusions with lower-concentration drugs. To achieve the latter, it will be necessary to apply more sophisticated techniques such as using multiple infusion catheters and computer modeling for targeted infusion[5,46] or brain-penetrating nanoparticles with regulated release.[55,56] These projects are ongoing, and results from clinical studies are eagerly awaited. To advance CED to an effective treatment strategy for pHGG including DIPG will be a clinical, biological, and technical challenge requiring a comprehensive multidisciplinary approach.

Conclusions

In vitro studies showed that anthracyclines, especially doxorubicin, are effective against pHGG and DIPG cells, while sparing normal human astrocytes. Convection-enhanced delivery can be used to achieve an adequate concentration of doxorubicin at the site of the tumor. However, preclinical evaluation of CED with free and liposomal doxorubicin showed that no therapeutic window could be reached in the pons to locally treat diffuse orthotopic brainstem tumors in mice because of excessive toxicity. The administration of higher-dose doxorubicin in orthotopic tumors within the thalamus was tolerated and effective in slowing down tumor growth. This preclinical study raises awareness that results obtained from supratentorial CED studies cannot be directly translated to the treatment of infratentorial tumors.

Acknowledgments

This research was made possible by the support of the Semmy Foundation, the Stichting Kika (Children-Cancer-free), and the Egbers Foundation.

References

1. Allard E, Passirani C, Benoit JP: Convection-enhanced delivery of nanocarriers for the treatment of brain tumors. **Biomaterials 30:**2302–2318, 2009
2. Anderson RCE, Kennedy B, Yanes CL, Garvin J, Needle M, Canoll P, et al: Convection-enhanced delivery of topotecan into diffuse intrinsic brainstem tumors in children. **J Neurosurg Pediatr 11:**289–295, 2013
3. Barenholz Y: Doxil®—the first FDA-approved nano-drug: lessons learned. **J Control Release 160:**117–134, 2012
4. Barua NU, Gill SS, Love S: Convection-enhanced drug delivery to the brain: therapeutic potential and neuropathological considerations. **Brain Pathol 24:**117–127, 2014
5. Barua NU, Lowis SP, Woolley M, O'Sullivan S, Harrison R, Gill SS: Robot-guided convection-enhanced delivery of carboplatin for advanced brainstem glioma. **Acta Neurochir (Wien) 155:**1459–1465, 2013
6. Boult JKR, Taylor KR, Vinci M, Popov S, Jury A, Molinari V, et al: Novel orthotopic pediatric high grade glioma xenografts evaluated with magnetic resonance imaging mimic human disease. **Cancer Res 75 (15 Suppl):**3271–3271, 2015 (Abstract)
7. Buczkowicz P, Hawkins C: Pathology, molecular genetics, and epigenetics of diffuse intrinsic pontine glioma. **Front Oncol 5:**147, 2015
8. Buczkowicz P, Hoeman C, Rakopoulos P, Pajovic S, Letourneau L, Dzamba M, et al: Genomic analysis of diffuse intrinsic pontine gliomas identifies three molecular subgroups and recurrent activating ACVR1 mutations. **Nat Genet 46:**451–456, 2014
9. Caretti V, Zondervan I, Meijer DH, Idema S, Vos W, Hamans B, et al: Monitoring of tumor growth and post-irradiation recurrence in a diffuse intrinsic pontine glioma mouse model. **Brain Pathol 21:**441–451, 2011
10. Chan KM, Fang D, Gan H, Hashizume R, Yu C, Schroeder M, et al: The histone H3.3K27M mutation in pediatric glioma reprograms H3K27 methylation and gene expression. **Genes Dev 27:**985–990, 2013
11. Chastagner P, Devictor B, Geoerger B, Aerts I, Leblond P, Frappaz D, et al: Phase I study of non-pegylated liposomal doxorubicin in children with recurrent/refractory high-grade glioma. **Cancer Chemother Pharmacol 76:**425–432, 2015
12. Chastagner P, Sudour H, Mriouah J, Barberi-Heyob M, Bernier-Chastagner V, Pinel S: Preclinical studies of pegylated- and non-pegylated liposomal forms of doxorubicin as radiosensitizer on orthotopic high-grade glioma xenografts. **Pharm Res 32:**158–166, 2015
13. Chittiboina P, Heiss JD, Warren KE, Lonser RR: Magnetic resonance imaging properties of convective delivery in diffuse intrinsic pontine gliomas. **J Neurosurg Pediatr 13:**276–282, 2014
14. Claes A, Schuuring J, Boots-Sprenger S, Hendriks-Cornelissen S, Dekkers M, van der Kogel AJ, et al: Phenotypic and genotypic characterization of orthotopic human glioma models and its relevance for the study of anti-glioma therapy. **Brain Pathol 18:**423–433, 2008
15. Di Leo A, Biganzoli L, Claudino W, Licitra S, Pestrin M, Larsimont D: Topoisomerase II alpha as a marker predicting anthracyclines' activity in early breast cancer patients: ready for the primetime? **Eur J Cancer 44:**2791–2798, 2008
16. Di Leo A, Gancberg D, Larsimont D, Tanner M, Jarvinen T, Rouas G, et al: HER-2 amplification and topoisomerase IIalpha gene aberrations as predictive markers in node-positive breast cancer patients randomly treated either with an anthracycline-based therapy or with cyclophosphamide, methotrexate, and 5-fluorouracil. **Clin Cancer Res 8:**1107–1116, 2002
17. Doyle L, Ross DD: Multidrug resistance mediated by the breast cancer resistance protein BCRP (ABCG2). **Oncogene 22:**7340–7358, 2003
18. Eisenstat DD, Pollack IF, Demers A, Sapp MV, Lambert P, Weisfeld-Adams JD, et al: Impact of tumor location and pathological discordance on survival of children with midline high-grade gliomas treated on Children's Cancer Group high-grade glioma study CCG-945. **J Neurooncol 121:**573–581, 2015
19. Fontebasso AM, Liu XY, Sturm D, Jabado N: Chromatin remodeling defects in pediatric and young adult glioblastoma: a tale of a variant histone 3 tail. **Brain Pathol 23:**210–216, 2013
20. Franklin KBJ, Paxinos G: **The Mouse Brain in Stereotaxic Coordinates, Compact Third Edition.** Cambridge, MA: Academic Press, 2008
21. Gaillard PJ, Appeldoorn CCM, Dorland R, van Kregten J, Manca F, Vugts DJ, et al: Pharmacokinetics, brain delivery, and efficacy in brain tumor-bearing mice of glutathione pegylated liposomal doxorubicin (2B3-101). **PLoS One 9:**e82331, 2014
22. Grasso CS, Tang Y, Truffaux N, Berlow NE, Liu L, Debily

MA, et al: Functionally defined therapeutic targets in diffuse intrinsic pontine glioma. **Nat Med 21:**555–559, 2015
23. Gravendeel LAM, Kouwenhoven MCM, Gevaert O, de Rooi JJ, Stubbs AP, Duijm JE, et al: Intrinsic gene expression profiles of gliomas are a better predictor of survival than histology. **Cancer Res 69:**9065–9072, 2009
24. Hargrave D, Chuang N, Bouffet E: Conventional MRI cannot predict survival in childhood diffuse intrinsic pontine glioma. **J Neurooncol 86:**313–319, 2008
25. Harris LW, Lockstone HE, Khaitovich P, Weickert CS, Webster MJ, Bahn S: Gene expression in the prefrontal cortex during adolescence: implications for the onset of schizophrenia. **BMC Med Genomics 2:**28, 2009
26. Jansen MH, Veldhuijzen van Zanten SE, Sanchez Aliaga E, Heymans MW, Warmuth-Metz M, Hargrave D, et al: Survival prediction model of children with diffuse intrinsic pontine glioma based on clinical and radiological criteria. **Neuro Oncol 17:**160–166, 2015
27. Jansen MHA, Kaspers GJ: A new era for children with diffuse intrinsic pontine glioma: hope for cure? **Expert Rev Anticancer Ther 12:**1109–1112, 2012
28. Jansen MHA, Lagerweij T, Sewing ACP, Vugts DJ, van Vuurden DG, Molthoff CFM, et al: Bevacizumab targeting diffuse intrinsic pontine glioma: results of 89Zr-bevacizumab PET imaging in brain tumor models. **Mol Cancer Ther 15:**2166–2174, 2016
29. Kakee A, Terasaki T, Sugiyama Y: Brain efflux index as a novel method of analyzing efflux transport at the blood-brain barrier. **J Pharmacol Exp Ther 277:**1550–1559, 1996
30. Kikuchi T, Saito R, Sugiyama S, Yamashita Y, Kumabe T, Krauze M, et al: Convection-enhanced delivery of polyethylene glycol-coated liposomal doxorubicin: characterization and efficacy in rat intracranial glioma models. **J Neurosurg 109:**867–873, 2008
31. Krauze MT, Noble CO, Kawaguchi T, Drummond D, Kirpotin DB, Yamashita Y, et al: Convection-enhanced delivery of nanoliposomal CPT-11 (irinotecan) and PEGylated liposomal doxorubicin (Doxil) in rodent intracranial brain tumor xenografts. **Neuro Oncol 9:**393–403, 2007
32. Lippens RJ: Liposomal daunorubicin (DaunoXome) in children with recurrent or progressive brain tumors. **Pediatr Hematol Oncol 16:**131–139, 1999
33. Lipshultz SE, Karnik R, Sambatakos P, Franco VI, Ross SW, Miller TL: Anthracycline-related cardiotoxicity in childhood cancer survivors. **Curr Opin Cardiol 29:**103–112, 2014
34. Lonser RR, Sarntinoranont M, Morrison PF, Oldfield EH: Convection-enhanced delivery to the central nervous system. **J Neurosurg 122:**697–706, 2015
35. Lonser RR, Warren KE, Butman JA, Quezado Z, Robison RA, Walbridge S, et al: Real-time image-guided direct convective perfusion of intrinsic brainstem lesions. Technical note. **J Neurosurg 107:**190–197, 2007
36. Morales La Madrid A, Hashizume R, Kieran MW: Future clinical trials in DIPG: bringing epigenetics to the clinic. **Front Oncol 5:**148, 2015
37. Pang B, Qiao X, Janssen L, Velds A, Groothuis T, Kerkhoven R, et al: Drug-induced histone eviction from open chromatin contributes to the chemotherapeutic effects of doxorubicin. **Nat Commun 4:**1908, 2013
38. Paugh BS, Broniscer A, Qu C, Miller CP, Zhang J, Tatevossian RG, et al: Genome-wide analyses identify recurrent amplifications of receptor tyrosine kinases and cell-cycle regulatory genes in diffuse intrinsic pontine glioma. **J Clin Oncol 29:**3999–4006, 2011
39. Paugh BS, Qu C, Jones C, Liu Z, Adamowicz-Brice M, Zhang J, et al: Integrated molecular genetic profiling of pediatric high-grade gliomas reveals key differences with the adult disease. **J Clin Oncol 28:**3061–3068, 2010
40. Qosa H, Miller DS, Pasinelli P, Trotti D: Regulation of ABC efflux transporters at blood-brain barrier in health and neurological disorders. **Brain Res 1628 (Pt B):**298–316, 2015
41. Saito R, Krauze MT, Noble CO, Tamas M, Drummond DC, Kirpotin DB, et al: Tissue affinity of the infusate affects the distribution volume during convection-enhanced delivery into rodent brains: implications for local drug delivery. **J Neurosci Methods 154:**225–232, 2006
42. Saito R, Sonoda Y, Kumabe T, Nagamatsu K, Watanabe M, Tominaga T: Regression of recurrent glioblastoma infiltrating the brainstem after convection-enhanced delivery of nimustine hydrochloride. **J Neurosurg Pediatr 7:**522–526, 2011
43. Salloum R, DeWire M, Lane A, Goldman S, Hummel T, Chow L, et al: Patterns of progression in pediatric patients with high-grade glioma or diffuse intrinsic pontine glioma treated with bevacizumab-based therapy at diagnosis. **J Neurooncol 121:**591–598, 2015
44. Schwartzentruber J, Korshunov A, Liu XY, Jones DTW, Pfaff E, Jacob K, et al: Driver mutations in histone H3.3 and chromatin remodelling genes in paediatric glioblastoma. **Nature 482:**226–231, 2012
45. Sewing ACP, Caretti V, Lagerweij T, Schellen P, Jansen MHA, van Vuurden DG, et al: Convection enhanced delivery of carmustine to the murine brainstem: a feasibility study. **J Neurosci Methods 238:**88–94, 2014
46. Siepmann J, Siepmann F, Florence AT: Local controlled drug delivery to the brain: mathematical modeling of the underlying mass transport mechanisms. **Int J Pharm 314:**101–119, 2006
47. Solomon DA, Wood MD, Tihan T, Bollen AW, Gupta N, Phillips JJJ, et al: Diffuse midline gliomas with histone H3-K27M mutation: a series of 47 cases assessing the spectrum of morphologic variation and associated genetic alterations. **Brain Pathol 26:**569–580, 2016
48. van Dalen EC, Raphaël MF, Caron HN, Kremer LCM: Treatment including anthracyclines versus treatment not including anthracyclines for childhood cancer. **Cochrane Database Syst Rev 9:**CD006647, 2014
49. van Tellingen O, Yetkin-Arik B, de Gooijer MC, Wesseling P, Wurdinger T, de Vries HE: Overcoming the blood-brain tumor barrier for effective glioblastoma treatment. **Drug Resist Updat 19:**1–12, 2015
50. Veringa SJE, Biesmans D, van Vuurden DG, Jansen MHA, Wedekind LE, Horsman I, et al: In vitro drug response and efflux transporters associated with drug resistance in pediatric high grade glioma and diffuse intrinsic pontine glioma. **PLoS One 8:**e61512, 2013
51. Wagner S, Peters O, Fels C, Janssen G, Liebeskind AK, Sauerbrey A, et al: Pegylated-liposomal doxorubicin and oral topotecan in eight children with relapsed high-grade malignant brain tumors. **J Neurooncol 86:**175–181, 2008
52. Wolff JE, Trilling T, Mölenkamp G, Egeler RM, Jürgens H: Chemosensitivity of glioma cells in vitro: a meta analysis. **J Cancer Res Clin Oncol 125:**481–486, 1999
53. Wu G, Broniscer A, McEachron TA, Lu C, Paugh BS, Becksfort J, et al: Somatic histone H3 alterations in pediatric diffuse intrinsic pontine gliomas and non-brainstem glioblastomas. **Nat Genet 44:**251–253, 2012
54. Zhang R, Saito R, Mano Y, Kanamori M, Sonoda Y, Kumabe T, et al: Concentration rather than dose defines the local brain toxicity of agents that are effectively distributed by convection-enhanced delivery. **J Neurosci Methods 222:**131–137, 2014
55. Zhou J, Patel TR, Sirianni RW, Strohbehn G, Zheng MQ, Duong N, et al: Highly penetrative, drug-loaded nanocarriers improve treatment of glioblastoma. **Proc Natl Acad Sci U S A 110:**11751–11756, 2013
56. Zhou Z, Ho SL, Singh R, Pisapia DJ, Souweidane MM:

Toxicity evaluation of convection-enhanced delivery of small-molecule kinase inhibitors in naïve mouse brainstem. **Childs Nerv Syst 31:**557–562, 2015

Disclosures

The authors report no conflict of interest concerning the materials or methods used in this study or the findings specified in this paper.

Author Contributions

Conception and design: Sewing, Lagerweij, van Vuurden, Kaspers. Acquisition of data: Sewing, Lagerweij, Meel, Veringa. Analysis and interpretation of data: Sewing, Wesseling. Drafting the article: Sewing. Critically revising the article: Lagerweij, van Vuurden, Vandertop, Wesseling, Kaspers, Hulleman. Reviewed submitted version of manuscript: Sewing, Lagerweij, Noske, Kaspers, Hulleman. Approved the final version of the manuscript on behalf of all authors: Sewing. Statistical analysis: Sewing, Veringa. Administrative/technical/material support: Meel, Carcaboso, Gaillard, Noske. Study supervision: Hulleman.

Supplemental Information

Online-Only Content

Supplemental material is available with the online version of the article.

Supplemental Figs. 1–3. https://thejns.org/doi/suppl/10.3171/2016.9.PEDS16152.

Previous Presentations

Portions of this work were presented in poster form at the Advances in Brain Cancer Research meeting held by the American Association for Cancer Research on May 27–30, 2015, in Washington, DC, and the 17th International Symposium on Pediatric Neuro-Oncology conference held on June 12–15, 2016, in Liverpool, United Kingdom.

Correspondence

A. Charlotte P. Sewing, VU University Medical Center, De Boelelaan 1117, CCA Rm. 3.56, 1081 HV Amsterdam, The Netherlands. email: a.sewing@vumc.nl.